ALTERNATIVE BEAM SPLITTER/COMPENSATOR CONFIGURATIONS FOR REDUCTION OF MULTIPLE REFLECTIONS IN IMAGING FOURIER TRANSFORM SPECTROMETERS

Justin D. Redd
Rocky Mountain NASA Space Grant Consortium
Utah State University, Logan, Utah

Abstract

Eight alternative beam splitter/compensator configurations for use in imaging infrared Fourier transform spectrometers are presented. The objective is to identify one or more configurations that may reduce multiple reflection problems in imaging Fourier transform spectrometers. The alternative configurations include: (1) dual slab with antireflection coatings, (2) dual slab at angles other than 45°, (3) dual slab with no air gap, (4) dual slab with widened air gap, (5) square 45° cube, (6) hexagonal 60° cube, (7) vertically stacked parallel slab, and (8) vertically stacked non-parallel slab. A description and brief analysis of each alternative configuration is included. The conclusion is that the dual slab with widened air gap configuration exhibits the best potential for reducing multiple reflections in imaging Fourier transform spectrometers.

I. Background

The techniques of Fourier Transform Spectroscopy using the Michelson interferometer have been in development since the 1950s.[1] The fundamentals of these techniques were well documented in the 1970 Aspen International Conference on Fourier Spectroscopy.[2]

The conventional Fourier Transform Spectrometer (FTS) splits incoming electromagnetic radiation into two nearly identical beams that travel different paths through the interferometer before recombining at a single detector [Figure 1]. One of the paths incorporates a movable mirror which allows its optical path length to be changed relative to the other path. The recombined beams interfere in an alternate constructive and destructive pattern as the optical path difference is varied from zero to some maximum. The resulting pattern of light and dark fringes incident upon the detector is called an *interferogram*. The Fourier transform of the interferogram yields the temporal frequency spectrum (which is the power spectral density function) of the incoming electromagnetic radiation.

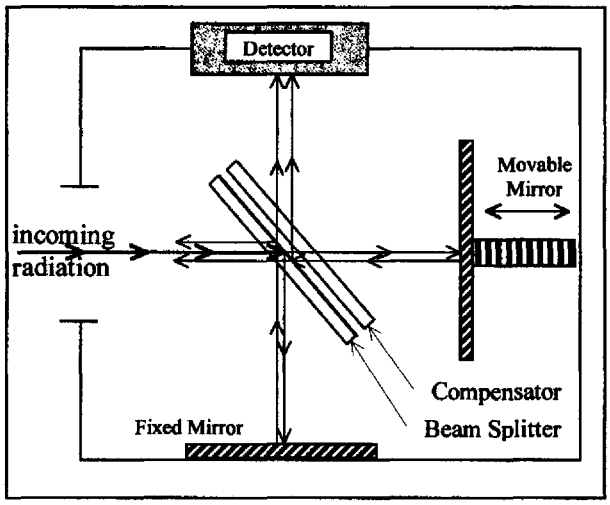

Figure 1. Michelson interferometer

The Utah State University Space Dynamics Laboratory is currently involved in extending the technique of Fourier transform spectroscopy by replacing the single detector with a 128 x 128 element detector array to produce an Imaging Fourier Transform

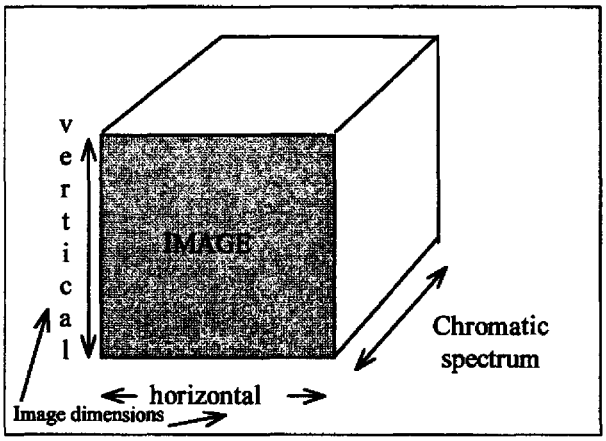

Figure 2. Hyperspectral data cube

Spectrometer (IFTS). The IFTS has the capability of collecting a separate interferogram at each pixel element of the focal plane detector array.

Fourier transformation of the array of interferograms results in a continuous set of discrete images, where each image in the set is formed by radiation at a distinct temporal frequency. This set of images is called a hyperspectral data cube [Figure 2].

II. The Multiple Reflection Problem

One of the obstacles in the process of engineering an IFTS is elimination of unwanted multiple reflections that occur within the beam splitter. The consequences of these reflections within the beam splitter are multiple offset images (ghosts) and multiple delayed interferograms (resulting in false spectral components in the power spectral density function).

A typical beam splitter used in infrared interferometry consists of two parallel slabs of calcium fluoride separated by a thin air gap[3] [Figure 3]. The first slab encountered by incident radiation is called the beam splitter, and the other is called the compensator. The beam splitter is coated on the back side with a thin layer of silicon. The boundary between the calcium fluoride (n = index of refraction = 1.42) and the silicon (n=3.44) is intended to reflect approximately 50% of the incident radiation and transmit the rest. The compensator is necessary to ensure that each of the two beams travel through the same total amount of dispersive material.

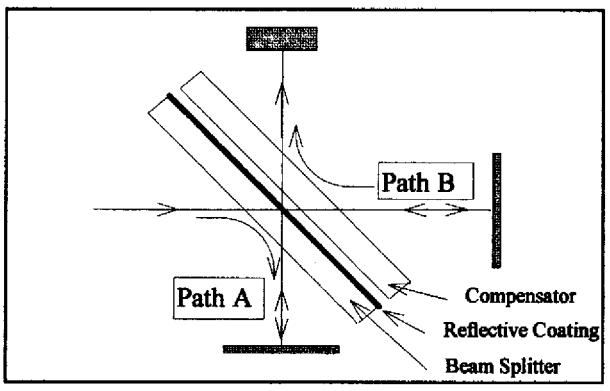

Figure 3. Dual slab beam splitter

The problem with this arrangement is that reflections also occur at every boundary between dissimilar materials. One pass through the beam splitter generates twelve secondary (unintentional) reflections at the air/calcium fluoride boundaries along with the three primary (intended) reflections at the calcium fluoride/silicon boundary of the beam splitter [Figure 4]. The twelve secondary reflections give rise to 47 tertiary reflections and so on.

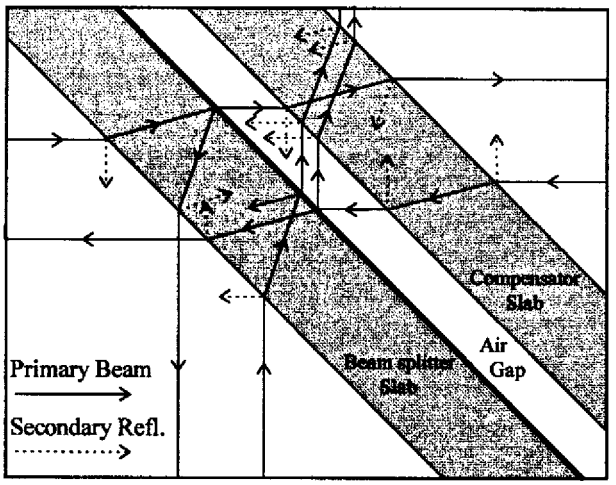

Figure 4. Primary and Secondary Reflections

Each of the unwanted secondary reflections affects the quality of the final spectral image by: (1) reducing the power in the primary beams, (2) potentially producing multiple offset images (ghosts) if the unwanted reflection is incident at the detector on the wrong pixel element, and (3) potentially producing false spectral components if the unwanted reflection is incident upon the detector and the reflection interferes with other primary or secondary incident radiation.

The negative effects of multiple reflections are more severe within imaging interferometers than within non-imaging interferometers. This is primarily due to the fact that non-imaging interferometers use a single detector, while imaging interferometers use an array of detectors. Multiple reflections are less likely to be incident upon a single detector. Also, unwanted multiple reflections that are incident on the single detector do not produce ghost images since single detector instruments are non-imaging. Finally, false spectral components that are produced in the power spectral density due to multiple reflections are a small fraction of the total power incident upon the single detector. This is in contrast to reflections incident upon individual imaging detector array elements which have less total power incident upon them. Typical non-imaging systems either ignore the effects of multiple reflections

or deal with the effects of multiple reflections after data collection using signal processing techniques.

III. Alternative Beam Splitter Configurations

The primary purpose of this paper is to identify alternative beam splitter/compensator configurations that should result in a reduction of unwanted reflections. The resulting alternative configurations will then be compared in future studies in order to optimize beam splitter performance in imaging infrared Fourier transform spectrometers.

The alternative beam splitter configurations have come from a variety of sources, including: discussions with experienced researchers in the field of Fourier transform spectroscopy[4], articles in the literature[5,6], and personal observation.

Analysis of each proposed configuration in this paper will be based on three comparison factors: (1) the number of unwanted secondary reflections, (2) the approximate volume relative the conventional configuration, and (3) the approximate weight relative the conventional configuration. A secondary reflection is defined as any unwanted reflection within the beam splitter that has a primary beam as its source. Tertiary reflections are unwanted reflections with secondary reflections as their source and so on.

The power carried by any reflection can be calculated by using the Fresnel equations:

$$R_{TE} = \frac{n_1 \cos\theta_1 - n_2 \cos\theta_2}{n_1 \cos\theta_1 + n_2 \cos\theta_2} \qquad (1)$$

$$R_{TM} = \frac{n_2 \cos\theta_1 - n_1 \cos\theta_2}{n_2 \cos\theta_1 + n_1 \cos\theta_2} \qquad (2)$$

where R_{TE} and R_{TM} are the amplitude reflection coefficients for transverse electric and transverse magnetic polarizations respectively, n_1 is the index of refraction of the material from which the radiation is coming, n_2 is the index of refraction of the material on which the radiation is incident, θ_1 is the angle of incidence, and θ_2 is the angle of refraction. The angle of refraction can be calculated from Snell's law, $n_1 \sin\theta_1 = n_2 \cos\theta_2$.

If the polarization is assumed random, then the overall amplitude reflection coefficient, R, can be approximated by assuming a 45° polarization, so that:

$$|R| = \sqrt{\frac{R_{TE}^2}{2} + \frac{R_{TM}^2}{2}} \qquad (3)$$

and the power reflection coefficient, Γ, is just the square of the amplitude coefficient:

$$\Gamma = |R|^2 \qquad (4)$$

The power transmission coefficient, T, is equal to 1- Γ.

Equations 1-4 can be applied at the air/calcium fluoride boundaries and at the calcium fluoride/air boundaries to calculate the power reflection coefficients. The power reflection coefficients range from 3 to 5% for radiation incident upon the beam splitter at angles in the 35 to 55° range. In order to simplify the analysis, the reflection coefficient at these boundaries will be assumed to have an average value of 4%. This approximation will be used, along with graphical ray tracing techniques to determine the number of secondary reflections and estimate their power.

A. Dual Slab with Antireflection Coatings

Antireflection (AR) coating techniques for large angles of incidence have been documented in the literature[7,8]. One possible solution to the multiple reflection problem is to use the conventional configuration [Figures 3 and 4] but incorporating an AR coating at each of the air/calcium fluoride boundaries. Assuming a field-widened interferometer[9] with a half-angle field of view of up to 10°, the AR coating would have to be effective at incidence angles of 45 ± 10° (35° to 55°).

The power reflection coefficient for randomly polarized radiation at an air/calcium fluoride boundary with no AR coating is approximately 4% over the 35 to 55° range of incidence angles. Half of the twelve secondary reflections that occur in a conventionally configured dual slab beam splitter will be incident at various pixel locations on the detector [Figure 4]. The percentage of the total infrared power carried by these six secondary reflections ranges between 0.3% and 1.8%. This figure was calculated by ray tracing each of the secondary reflections through to the detector with 4% of the power reflected at each boundary. Assuming that the detector outputs are digitized to at least 12 bits, a single bit represents $1/2^{12} = 1/4096 = 0.02\%$.

To reduce the power of the secondary reflections to the level of one bit would require an AR coating that reduces the power reflection at the air/calcium fluoride interface from 4% to approximately (4%)(.02%) / (1.8%) ≈ 0.04%. This represents a factor of 100 reduction. While any reduction in reflection would be beneficial, an AR coating that would solve the multiple reflection problem (by reducing reflections by a factor of 100 at large angles of incidence) will be difficult to obtain.

B. Dual Slab at Angles other than 45°

If the conventional dual slab configuration is oriented so that the angle of incidence of on-axis rays is other than 45°, the number of secondary reflections is unchanged. This can be seen by referring to Figure 4 and postulating that secondary reflections exist at the same locations regardless of changes in the beam splitter angle. Varying the angle of incidence does influence the magnitude of the power reflection coefficient, however, so that the negative effects of the secondary reflections can be increased or decreased to some degree.

At near grazing incidence (almost 90°), the reflection coefficient approaches 100%. Even if the angles of incidence are in the 75° range, the reflection coefficient is approximately 24%. Also, at large angles of incidence, AR coatings which function properly are more difficult to achieve. For these reasons, increasing the angle of incidence can be detrimental to beam splitter performance.

At smaller angles of incidence (0-40°), however, the opposite is the case: the reflection coefficient approaches a minimum, and AR coatings for close to normal incidence can be achieved. For incidence angles between normal (0°) and 40°, the reflection coefficient is approximately constant at a value of 3%. Decreasing the incidence angle from 45 to 30° would result in a reduction of power in the secondary reflections from 4 to 3%, for an approximate improvement of 1%/4% = 25%. While an improvement of this magnitude is significant, it does not represent a complete solution to the multiple reflection problem.

C. Dual Slab with no Air Gap

The primary reason for the air gap in a conventional dual slab beam splitter/compensator is that manufacturing difficulties are associated with its elimination. Reports in the literature, however, indicate that practical methods of eliminating the air gap do exist[10]. Figure 4 shows that four of the twelve secondary reflections occur within the air gap. Elimination of the air gap would reduce the number of secondary reflections from twelve to eight. While this is significant, it is not a complete solution to the multiple reflection problem.

D. Dual Slab with Widened Air Gap

The dual slab with widened air gap configuration is similar to the conventional configuration of Figure 3, except that the air gap has been widened so that the horizontal gap width is approximately the same as the projection of the slab surface onto the horizontal axis [Figure 5]. The same secondary reflections which exist in the conventional configuration also exist in this one, but the change in dimensions of the air gap causes the secondary reflections to miss the detector.

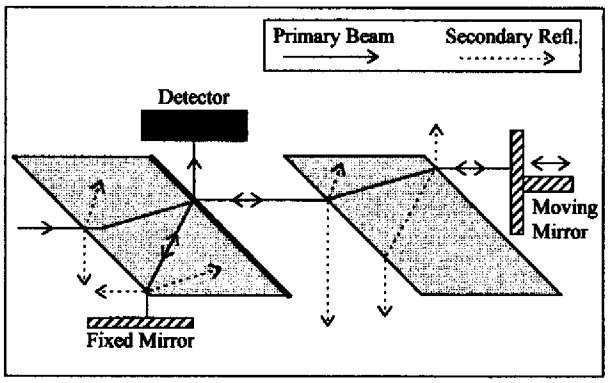

Figure 5. Dual Thick Slab with Widened Air Gap

This solution to the multiple reflection problem warrants further study since none of the secondary reflections are incident upon the detector. The weight of this configuration is the same as the conventional configuration, but it requires approximately 70% more volume.

E. Square 45° Cube

The square cube beam splitter with 45° incidence angle and no air gap is another potential solution to the multiple reflection problem [Figure 6]. Fabrication techniques for this configuration (composed of two prisms) are detailed in a paper by K.B. Farr and N. George[10]. The total volume occupied by the cube beam splitter is approximately the same as with the conventional dual slab arrangement. More of the volume is

filled with the calcium fluoride, however, resulting in a weight increase of approximately 66%.

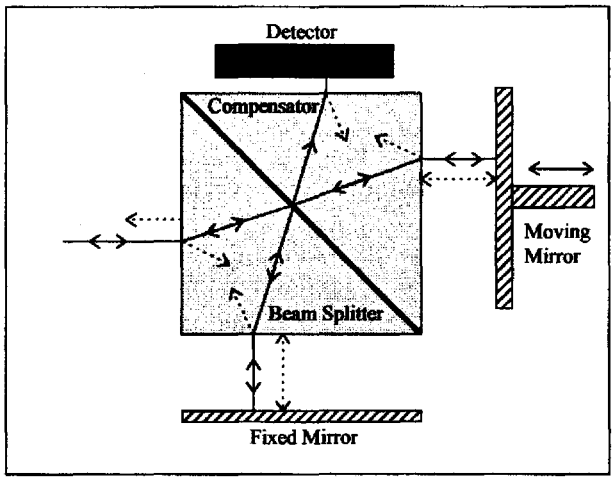

Figure 6. Square 45° Cube

Secondary reflections in the square cube beam splitter occur in four locations: (1) at the cube surface where radiation is first incident, (2) at the cube surface facing the fixed mirror, (3) at the cube surface facing the movable mirror, and (4) at the cube surface facing the detector. At the first three of these locations there are two secondary reflections: one external to the cube and one internal to the cube. At the fourth location, there is only an internal secondary reflection. The total number of secondary reflections is seven, and only the external reflection at the first location can be dismissed as inconsequential. The other six secondary reflections will potentially have detrimental effects, which is no better than the original dual slab configuration.

F. Hexagonal 60° Cube

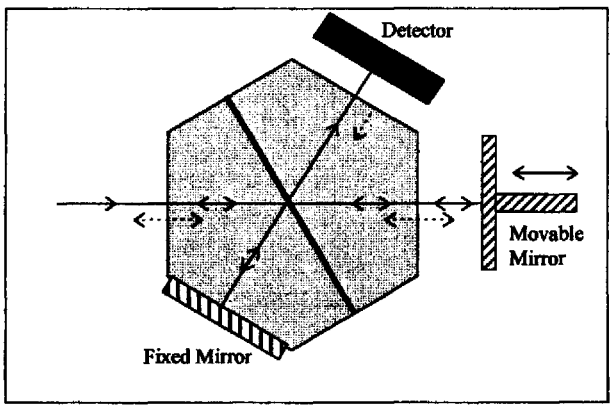

Figure 7. Hexagonal 60° cube beam splitter

An hexagonal 60° cube beam splitter with no air gap is shown in Figure 7. The fixed mirror is assumed to be in direct contact with the cube. A thorough analysis of this design is contained in a paper by J.A. Dobrowolski et al[11]. From Figure 7 it can be seen that the hexagonal beam splitter suffers from five secondary reflections, and four of the five will potentially be incident on the detector. The hexagonal design also has 2.6 times the volume and 4.3 times the weight of the conventional configuration.

G. Vertically Stacked Parallel Slab

The vertically stacked parallel slab beam splitter consists of two parallel slabs of dimensions similar to the conventional parallel slab configuration [Figure 8]. The differences are: (1) the silicon/calcium fluoride beam splitting boundary is on the leading surface of the beam splitter slab, (2) the air gap is large (on the order of the height of the beam splitter slab projected onto the vertical axis), and (3) the compensator slab is positioned below the beam splitter slab instead of behind it.

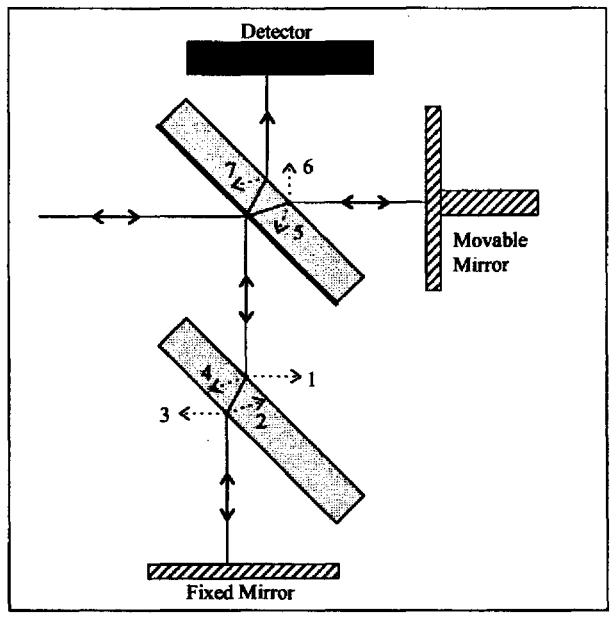

Figure 8. Vertically stacked parallel slab

There are seven secondary reflections in this configuration (numbered in Figure 8). The first four will not be incident upon the detector, but the last three will. In particular, secondary reflections six and seven will contain relatively large amounts of power and result in multiple reflection problems. The volume of this arrangement is approximately 63% larger than the

conventional configuration, but the weight is approximately the same.

H. Vertically Stacked Non-parallel Slab

The vertically stacked non-parallel slab arrangement is identical to the vertically stacked parallel slab beam splitter except that the compensator slab is parallel to the fixed mirror instead of parallel to the compensator. The compensator thickness must be equal to the length of the optical path traveled in the beam splitter slab [Figure 9]. Also, the fixed mirror can be in contact with the compensator.

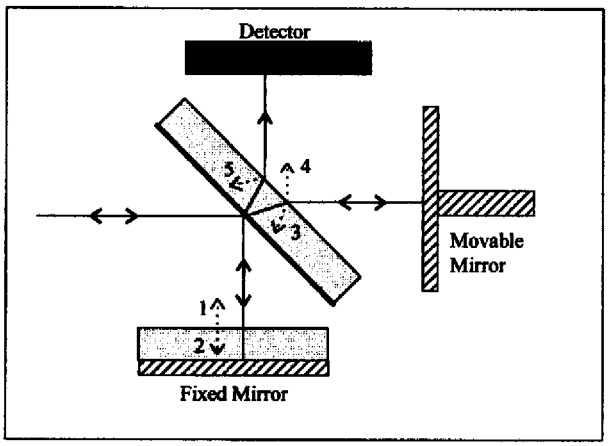

Figure 9. Vertically stacked non-parallel slab

There are five secondary reflections in this configuration (numbered in Figure 9) versus seven in the vertically stacked parallel slab. All five will eventually be incident upon the detector, however, as compared with three in the previous arrangement. In particular, secondary reflections four and five will carry relatively large amounts of infrared power, but all five will result in multiple reflection problems. The volume of this arrangement is approximately 20% larger than that of the conventional configuration, but the weight is approximately the same.

IV. Conclusions

Each of the eight alternative beam splitter configurations presented above have strengths and weaknesses relative to the traditional beam splitter configuration for infrared two-beam interferometers. The only configuration that offers the possibility of complete elimination of unwanted multiple reflections is the dual slab with widened air gap.

An additional advantage possessed by the dual slab with widened air gap configuration is that it can be constructed using the same optical components as the traditional configuration. The mounting structure would have to be changed to accommodate the widened air gap and additional beam splitter volume would be necessary.

The dual slab with widened air gap configuration for the beam splitter/compensator has definite potential for solving the multiple reflection problem and warrants further study.

Acknowledgments

This work was supported by the Rocky Mountain NASA Space Grant Consortium and by the Utah State University Space Dynamics Laboratory. A special thanks to Doran Baker, Ronald Huppi, Mark Esplin, and Roy Esplin for excellent advise and encouragement.

References

[1] D. Baker, A. Steed, and A.T. Stair, Jr., "Development of infrared interferometry for upper atmospheric emission studies," *Applied Optics*, vol. 20, no. 10, pp. 1734-1746, May 1981.

[2] "Proceedings of the Aspen international conference on Fourier spectroscopy, 1970," G.A. Vanasse, A.T. Stair Jr., and Doran J. Baker, editors, U.S Air Force document AFCRL-71-0019, 5 Jan. 1971.

[3] A.G. Tescher, "Beam splitter optimization for fourier spectroscopy," in *Proceedings of the Aspen International Conference on Fourier Spectroscopy*, pp. 225-230, April 1971.

[4] Various discussions with Mark Esplin and Ronald Huppi of the Stewart Radiance Laboratory as well as with Allan Steed and staff of the Space Dynamics Laboratory.

[5] J.A. Dobrowolski, F.C. Ho, and A. Waldorf, "Beam splitter for a wide-angle Michelson Doppler imaging interferometer," *Applied Optics*, vol. 24, no. 11, pp. 1585-1588, June 1985.

[6] T.W. Liepmann, "Wedged plate beam splitter without ghost reflections," *Applied Optics*, vol. 31, no. 28, pp. 5905-5906, Oct. 1992.

[7] A. Premoli and M.L. Rastello, "Minimax refining of wideband antireflection coatings for wide angular incidence," *Applied Optics*, vol. 33, no. 10, pp. 2018-2024, Apr. 1994.

[8] J. Monga, "Double-layer broadband antireflection coatings for grazing incidence angles," *Applied Optics*, vol. 31, no. 4, pp. 546-553, Feb. 1992.

[9] D.J. Baker, "Field-widened interferometers for Fourier spectroscopy," *Spectrometric Techniques, vol. 1*, G.A. Vanasse, editor. New York, N.Y., Academic Press, 1977.

[10] K.B. Farr and N. George, "Beamsplitter cube for white light interferometry," *Applied Optics*, vol. 31, no. 10, pp. 2191-2196, Oct. 1992.

[11] J.A. Dobrowolsi, F.C. Ho, and A. Waldorf, "Beam splitter for a wide-angle Michelson Doppler imaging interferometer," *Applied Optics*, vol. 24, no. 11, pp. 1585-1588, Jun. 1985.